

Effective Multi-Graph Neural Networks for Illicit Account Detection on Cryptocurrency Transaction Networks

Zhihao Ding, Jieming Shi, *Member, IEEE*, Qing Li, *Fellow, IEEE*, Jiannong Cao, *Fellow, IEEE*

Abstract—We study illicit account detection on transaction networks of cryptocurrencies that are increasingly important in online financial markets. The surge of illicit activities on cryptocurrencies has resulted in billions of losses from normal users. Existing solutions either rely on tedious feature engineering to get handcrafted features, or are inadequate to fully utilize the rich semantics of cryptocurrency transaction data, and consequently, yield sub-optimal performance. In this paper, we formulate the illicit account detection problem as a classification task over directed multigraphs with edge attributes, and present **DIAM**, a novel multi-graph neural network model to effectively detect illicit accounts on large transaction networks. First, **DIAM** includes an Edge2Seq module that automatically learns effective node representations preserving intrinsic transaction patterns of parallel edges, by considering both edge attributes and directed edge sequence dependencies. Then utilizing the multigraph topology, **DIAM** employs a new Multigraph Discrepancy (MGD) module with a well-designed message passing mechanism to capture the discrepant features between normal and illicit nodes, supported by an attention mechanism. Assembling all techniques, **DIAM** is trained in an end-to-end manner. Extensive experiments, comparing against 14 existing solutions on 4 large cryptocurrency datasets of Bitcoin and Ethereum, demonstrate that **DIAM** consistently achieves the best performance to accurately detect illicit accounts, while being efficient. For instance, on a Bitcoin dataset with 20 million nodes and 203 million edges, **DIAM** achieves F1 score 96.55%, significantly higher than the F1 score 83.92% of the best competitor. The code is available at <https://github.com/TommyDzh/DIAM>.

Index Terms—Multigraphs, Graph Neural Networks, Illicit Account Detection, Transaction Networks, Cryptocurrency.

I. INTRODUCTION

ONLINE payment and exchange platforms are playing a growing role in financial markets [1]–[5]. Massive online transaction data have been generated. In general, a transaction network can be modeled as a *directed multigraph* that permits multiple edges between nodes (*i.e.*, multiple transactions between accounts) and allows *edge attributes* that describe the corresponding transactions (*e.g.*, transaction timestamp and amount). Figure 1 shows an example transaction network. Edge e_{10} is a transaction from nodes v_6 to v_7 with transaction timestamp and transaction amount as edge attributes (edge

attributes of other edges are omitted for brevity in Figure 1). Multiple edges can exist between nodes. For instance, edges e_4, e_5, e_6 between nodes v_3 and v_4 in Figure 1 represent three transactions that have happened between v_3 and v_4 . A node (*e.g.*, v_4) can have in and out transactions.

In recent years, one representative type of online transactions, cryptocurrency, has become increasingly popular and important, due to the nature of decentralization and pseudo-anonymity based on blockchain technology. As of February 2023, Bitcoin and Ethereum are the top-2 largest cryptocurrencies with \$650 billion market capitalization in total [6]. An Ethereum transaction is a message sent from a sender address¹ to a receiver address at certain time with certain transaction amount, forming a directed edge. Bitcoin is slightly complicated by allowing multiple senders and receivers in a transaction. Both of them can be modeled by the multigraph model in Figure 1 (see Section III-A).

Albeit the huge volume of cryptocurrency transactions generated by normal users, illicit entities are also taking advantage of Bitcoin and Ethereum for illegal activities, such as phishing scams [7]–[10], Ponzi scheme [7], [11], ransomware [12], and money laundering [13], which put millions of normal users at the risk of financial loss and hinder the development of blockchain ecosystem. In fact, cryptocurrency-related illicit activities are recognized as one of the fastest-growing cyber-crimes [12], *e.g.*, a reported surge of scamming revenue increasing by 82% in 2021, resulting to \$7.8 billion loss from victims [14]. Therefore, it is of great importance to develop effective methods to identify the illicit accounts on transaction networks of cryptocurrencies, including Bitcoin and Ethereum, which is the focus of this paper.

However, it is a highly challenging task to accurately detect illicit accounts, particularly on large-scale transaction networks with massive number of transactions. Cryptocurrency accounts are anonymous, and thus, there exists no meaningful portrait information as node features that are crucial to detect illicit accounts. Also illicit accounts can deliberately provide meaningless user data and transactions to hide. For instance, in Figure 1, there are 2 illicit (v_4 and v_5) and 5 benign nodes. All of them are connected by transactions, and apparently it is non-trivial to distinguish the two classes of nodes. Moreover, the directed multigraph with edge attributes is inherently sophisticated as shown in Figure 1, which makes it hard to develop a

Zhihao Ding is with the Department of Computing, The Hong Kong Polytechnic University E-mail: 22040455R@connect.polyu.hk.

Jieming Shi is with the Department of Computing, The Hong Kong Polytechnic University. E-mail: jieming.shi@polyu.edu.hk.

Qing Li is with the Department of Computing, The Hong Kong Polytechnic University. E-mail: csqli@comp.polyu.edu.hk.

Jiannong Cao is with the Department of Computing, The Hong Kong Polytechnic University. E-mail: csjcao@comp.polyu.edu.hk.

¹Account, address, and node are used interchangeably.

synergetic model that exploits all available feature dimensions over the multigraph topology for effective detection.

A collection of existing solutions [7], [10]–[12] mainly rely on feature engineering to extract handcrafted features by aggregating cryptocurrency transaction information (e.g., total amount received [7], [10]). Such shallow statistical features highly depend on domain expertise and overlook the hidden transaction patterns expressed in the multigraph data model. There are also studies using Graph Neural Networks (GNNs) for detection [8]–[10], [13], [15]. However, simple adoption of common GNNs, such as GCNs [16] and GATs [17], may not capture the unique characteristics of illicit accounts. In particular, traditional GNNs mainly rely on the homophily assumption that connected nodes share similar representations [18], which, however, is not true for illicit account detection. In Figure 1, nodes v_4 and v_3 are connected, but they should have very different representations since v_4 is illicit while v_3 is normal. In other words, the representations of connected nodes can have a very large *discrepancy* in illicit account detection (also known as inconsistency in [19]–[21]). Existing cryptocurrency studies with simple adoption of common GCNs and GATs that are not aware of the discrepancy may learn indistinguishable node representations. As reviewed in Section II-B, there are also studies on general graph-based anomaly detection [22], [23]. These methods can be customized for the problem of illicit account detection, but yield moderate performance in experiments.

In this paper, we study the problem of Detecting Illicit Accounts as a node classification task on directed Multigraphs with edge attributes, for transaction networks of cryptocurrencies. We present DIAM, a multi-graph neural network method for effective illicit account detection. DIAM consists of several well-thought-out technical designs to holistically utilize all of directed multigraph topology, edge attributes, and parallel edge sequential dependencies. First, DIAM has an *Edge2Seq* module that automatically learns high-quality representations to preserve the intrinsic transaction patterns represented by the directed parallel edges with attributes. Specifically, *Edge2Seq* adopts Recurrent Neural Networks (RNNs) to model and capture both edge attributes and edge sequence dependencies into node representations. Note that *Edge2Seq* handles incoming and outgoing edges of a node separately since a node can have significantly different transaction patterns when being a sender/receiver [7]. To further utilize the multigraph topology and handle the discrepancy issue mentioned above, we then develop an *Multigraph Discrepancy (MGD)* module in DIAM. MGD is a well-designed message passing mechanism to propagate not only node representations, but also the discrepancies between nodes, along directed multiple edges, with the help of a dedicated attention mechanism and learnable transformation. In other words, MGD can preserve both similar and discrepant features, which are vital for effective illicit account detection. DIAM stacks multiple MGD modules to consider multi-hop multigraph topology. Finally, assembling all techniques, DIAM is trained in an end-to-end manner, to minimize a cross-entropy loss. We evaluate DIAM against 14 existing solutions over 4 real cryptocurrency datasets of Bitcoin and Ethereum. Extensive experiments validate that DIAM

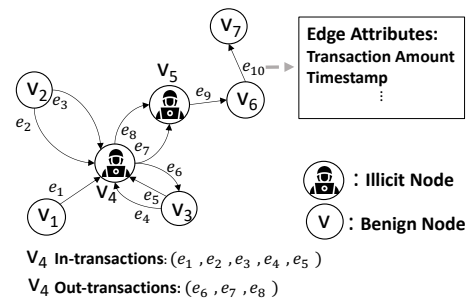


Fig. 1. An example of a directed multigraph with edge attributes for transaction networks. All edges (e.g., e_{10}) have attributes such as transaction amount and timestamp. v_4 and v_5 are illicit, while the others are normal. The in and out transactions of v_4 are listed.

consistently achieves the highest accuracy on all datasets, outperforming competitors often by a significant margin, while being efficient.

Summing up, our contributions are as follows:

- We study the problem of illicit account detection on transaction networks of cryptocurrencies, and present DIAM, an effective multi-graph neural network over large directed multigraphs with edge attributes.
- In DIAM, we develop an *Edge2Seq* module that automatically learns and captures edge attributes, edge sequence dependencies, and edge directions into expressive node representations.
- We further design MGD, a multigraph discrepancy module to effectively preserve the representation discrepancies between illicit and benign nodes over the multi-hop multigraph topology.
- The superiority of DIAM is validated via extensive experiments by comparing 14 baselines on 4 real datasets.

II. RELATED WORK

Our work is closely related to studies on cryptocurrency illicit account detection, and graph-based anomaly detection.

A. Cryptocurrency Illicit Account Detection

As mentioned, there is a lack of meaningful portrait information as node features for cryptocurrency illicit account detection. Early studies mostly rely on tedious feature engineering to obtain shallow statistical features, such as the sum, average, standard deviation of transaction amounts and time [7], [8], [10]. These studies then mainly employ on-the-rack classifiers (e.g., XGBoost [24] and LightGBM [25]) over the extracted features to detect illicit accounts [7], [8], [12]. To further exploit the graph topological characteristics of cryptocurrency transaction networks, recent studies [9], [10] incorporate network embedding techniques for illicit account detection. For instance, Poursafaei *et al.*, [10] use *node2vec* [26] and *Ri-walk* [27] to extract structural information from different views into node embeddings, and further leverage extracted features, for the training process of illicit account detection. Wu *et al.*, [9] propose *trans2vec*, which is a random-walk based node embedding method, in which, the random walk transition probability is biased by transaction amounts and time. However, these studies still partially rely on handcrafted

node features, and do not fully exploit the multigraph data model of cryptocurrency transactions. With the success of GNNs, latest studies start to use GNNs on cryptocurrency transaction networks, *e.g.*, [8], [13], [15], [28]. Weber *et al.*, [13] train an end-to-end GCN for anti-money laundering in Bitcoin. Tam *et al.*, [15] propose EdgeProp that augments edge attributes in the message passing mechanism to identify illicit accounts in Ethereum. Li *et al.*, [28] incorporate GNNs and self-supervised learning to detect phishing scams. Summing up, most of existing cryptocurrency illicit account detection methods still adopt manual feature engineering for node feature initialization [7], [8], [10]–[13]. Moreover, existing studies did not explicitly design techniques to fully utilize the rich semantics of directed multigraph data model for illicit account detection [9], [10], [15]. In this work, we exploit the directed multigraph data model, and develop dedicated techniques to automatically learn deep intrinsic node representations that are highly effective for illicit account detection on cryptocurrency transaction networks.

B. Graph-based Anomaly Detection

In literature, there exist anomaly detection methods on various types of graph-based data, *e.g.*, review graphs [15], [19], [23], [29]. Most of the recent graph-based anomaly detection methods are under the regime of GNNs. Classic GNNs, such as GCN [16], Sage [30], and GAT [17], rely on the assumption of homophily [31]. That is, similar nodes tend to connect to each other, which is not true in anomaly detection. GINE [32] and TransConv [33] attempt to incorporate edge features in GNNs, but still follows the homophily assumption. Abnormal nodes usually have discrepant features, compared with normal ones [20]. Further, abnormal nodes often intentionally create connections with normal nodes to hide in camouflage [19]. Therefore, classic GNNs may not be able to effectively handle these issues for anomaly detection. To alleviate the issues, CARE-GNN [19] trains a predictor to measure the similarity between target nodes and their neighborhoods, and further leverage reinforcement learning to find the most related neighbors for aggregation. In [34], a new framework is proposed to use attention mechanism and generative adversarial learning [35] to detect anomalies. Zhou *et al.*, enhance vanilla GNNs with subtractive aggregation to model camouflage behaviors [36]. In [37], a new loss function that leverages global structure patterns for generating anomaly-detectable representations is presented. Liu *et al.*, [38] propose PC-GNN to sample neighbors from the same class and relieve the imbalance between abnormal and normal nodes. Ding *et al.*, [22] leverage meta-learning, while Wang *et al.*, [21] use self-supervised learning in GNNs, for detection. FRAUDRE [39] takes mean aggregation of neighborhood differences and representations, and develops a loss function to remedy class imbalance for anomaly detection. These methods can be customized for the illicit account detection problem. We have a detailed discussion in Section IV-C to elaborate the technical differences between our MGD technique and existing methods that also consider the discrepancy issue. In experiments, we compare with existing graph-based anomaly detection methods

TABLE I
FREQUENTLY USED NOTATIONS

Notation	Description
G (V, E, \mathbf{X}_E)	A directed multigraph with node set V , edge set E , and edge attribute matrix \mathbf{X}_E .
$N_{in}(v), N_{out}(v)$	The multisets of node v 's incoming and outgoing neighbors, respectively.
$Y_{\mathcal{L}}, Y_{\mathcal{U}}$	The sets of observed and unobserved node labels, respectively.
X_v^{out}, X_v^{in}	The incoming and outgoing edge attribute sequences of node v , respectively.
$\mathbf{h}_{v_{in}}, \mathbf{h}_{v_{out}}$	The incoming and outgoing sequence representation of node v , respectively.
\mathbf{h}_v	The node representation concatenating $\mathbf{h}_{v_{in}}$ and $\mathbf{h}_{v_{out}}$ of node v .
$\mathbf{z}_v^{(\ell)}$	The linearly transformed node representation of node v at ℓ -th MGD.
$\mathbf{r}_{v_{in}}^{(\ell)}, \mathbf{r}_{v_{out}}^{(\ell)}$	The discrepancy-aware incoming and outgoing messages node v received at ℓ -th MGD, respectively.
$\alpha_{v,1}, \alpha_{v,2}, \alpha_{v,3}$,	The attention weights of $\mathbf{z}_v^{(\ell)}, \mathbf{r}_{v_{in}}^{(\ell)}, \mathbf{r}_{v_{out}}^{(\ell)}$, respectively.
$\mathbf{h}_v^{(\ell)}$	Node representation after ℓ -th MGD of node v .
T_{\max}	Maximum length of edge attribute sequences.
d	The dimension of edge attributes.
c	The dimension of hidden representations.
L	The number of MGD layers.

to evaluate the effectiveness. In summary, these methods are designed without considering the aforementioned unique characteristics of cryptocurrency transactions, such as lack of meaningful node features. Moreover, they are designed either for relation graphs (*e.g.*, [19], [38], [39]) or node-attributed graphs (*e.g.*, [21], [34]). On the other hand, we consider all aspects of the multigraph data model into DIAM for illicit account detection.

III. PRELIMINARIES

We first present the data model of directed multigraph with edge attributes, to depict real-world transaction networks, and then provide the definition of the illicit account detection problem as a classification task on the data model.

A. Directed Multigraphs With Edge Attributes

Transactions can be treated as the interactions among accounts. Here we focus on how to build directed multigraphs with edge attributes using transaction data, and adopt Ethereum and Bitcoin transactions to explain. For interested readers, see [40] for a comprehensive introduction of Bitcoin and Ethereum. A transaction e sent from accounts v to u can be regarded as a directed edge from nodes v to u with edge attributes describing transaction details, such as transaction amount and timestamp (*e.g.*, edge e_{10} in Figure 1). Parallel edges may exist between v and u , since there could be many transactions between nodes v and u . Ethereum transactions follow the procedure above to model transactions into multigraphs. Bitcoin transactions are similar but with differences. Specifically, a Bitcoin transaction can contain multiple senders

and receivers who may send or receive different amounts of Bitcoin respectively in the transaction [41]. Given a Bitcoin transaction, we will create a directed edge e from every sender v to every receiver u in the transaction, and edge attributes contain the amount sent by v , the amount received by u , timestamp, and other related information, *e.g.*, transaction fee.

Given a collection of transactions, we can build the corresponding directed multigraph with edge attributes, by following the steps above. Specifically, let $G = (V, E, \mathbf{X}_E)$ be a directed multigraph, consisting of (i) a node set V that contains n nodes, (ii) a set of directed edges E of size m , each connecting two nodes in V , and (iii) an edge attribute matrix $\mathbf{X}_E \in \mathbb{R}^{m \times d}$, each row of which is a d -dimensional vector serving as the edge attributes to encode the details of the corresponding transaction. In a multigraph G , nodes v and u can have parallel edges with different edge attributes. Let $N_{out}(v)$ be the *multiset* of node v 's outgoing neighbors. If a node u has many transactions received from v , u will have multiple occurrences in $N_{out}(v)$. Similarly, let $N_{in}(v)$ be the *multiset* of node v 's incoming neighbors.

B. Problem Definition

Given a directed multigraph $G = (V, E, \mathbf{X}_E)$ with a subset of V containing labeled nodes, where each labeled node v has a class label $y_v \in \{0, 1\}$, indicating v is illicit ($y_v = 1$) or benign ($y_v = 0$), we formulate the problem of illicit account detection on directed multigraphs with edge attributes as a classification task defined as follows.

Definition 1: (Illicit Account Detection on Directed Multigraphs.) Given a partially labeled directed multigraph $G = (V, E, \mathbf{X}_E, Y_{\mathcal{L}})$, where $Y_{\mathcal{L}}$ is the set of the partially observed node labels, and each node label $y_v \in Y_{\mathcal{L}}$ takes value either 1 or 0, indicating the node to be illicit or not, the objective is to learn a binary classifier f that can accurately detect the illicit accounts in $Y_{\mathcal{U}}$:

$$f : G = (V, E, \mathbf{X}_E, Y_{\mathcal{L}}) \mapsto Y_{\mathcal{L}} \cup Y_{\mathcal{U}}, \quad (1)$$

where $Y_{\mathcal{U}}$ is the set of unobserved node labels to be predicted in G .

As mentioned, we use representative cryptocurrencies, Bitcoin and Ethereum transactions, as instances to elaborate and evaluate our method. Bitcoin and Ethereum are distributed public ledgers that record all transactions anonymously accessible to the public [8], [42]. Further, in terms of labeled data $Y_{\mathcal{L}}$, since the addresses in cryptocurrency platforms are unique and immutable, there are websites and forums, like WalletExplorer [43] and EtherScan [44], providing illicit label information over addresses involving illicit activities, such as phishing and gambling. As described in Section V-A, we crawl such information as ground-truth labels.

Table I lists the frequently used notations in the paper.

IV. THE DIAM FRAMEWORK

In this section, we present our solution DIAM. We provide the overview in Section IV-A, develop the Edge2Seq module to learn representations over directed parallel edges with

attributes in Section IV-B, design the MGD module that considers multigraph topology and representation discrepancies in Section IV-C, and elaborate the objective and algorithmic analysis of DIAM in Section IV-D.

A. Solution Overview

Figure 2 presents the proposed DIAM framework. Taking as input a directed multigraph G with edge attributes, which models a transaction network, the first module in DIAM is Edge2Seq that automatically learns expressive representations with the consideration of both incoming and outgoing edges of nodes. In particular, as shown in Figure 2, for a node v (*e.g.*, v_4), Edge2Seq first builds an incoming sequence X_v^{in} and an outgoing sequence X_v^{out} that consist of v 's incoming and outgoing edge attributes in chronological order, respectively. Intuitively, X_v^{out} and X_v^{in} describe different sequential transaction patterns of node v , when v serves as a sender or a receiver respectively. Then Edge2Seq employs an RNN model, specifically Gated Recurrent Units (GRUs) [45], to learn the sequence representations of both X_v^{out} and X_v^{in} , which are then processed by pooling operations, to get representations $\mathbf{h}_{v_{out}}$ and $\mathbf{h}_{v_{in}}$ respectively. Then as shown in Figure 2, $\mathbf{h}_{v_{out}}$ and $\mathbf{h}_{v_{in}}$ are concatenated together to be the node representation \mathbf{h}_v of v . Intuitively, \mathbf{h}_v captures both the incoming and outgoing transaction patterns of node v , as well as their sequential dependencies. The node representations \mathbf{h}_v for all $v \in V$ learned by Edge2Seq are then regarded as initial inputs fed into the proposed multigraph discrepancy (MGD) module. DIAM stacks multiple MGD layers to further consider multi-hop multigraph topology to learn more expressive discrepancy-aware node representations. In an MGD, a target node v receives messages from its incoming and outgoing neighborhoods separately (*e.g.*, v_4 as an example in MGD of Figure 2). The incoming and outgoing messages, denoted as $\mathbf{r}_{v_{in}}$ and $\mathbf{r}_{v_{out}}$, contain *both* neighbor representations and their *discrepancies* with the target node as shown in Figure 2, in order to preserve distinguishable features for illicit account detection. Then an attention mechanism is designed in MGD to integrate v 's representation \mathbf{z}_v , incoming message $\mathbf{r}_{v_{in}}$, and outgoing message $\mathbf{r}_{v_{out}}$ together via attentions $\alpha_{v,1}$, $\alpha_{v,2}$, and $\alpha_{v,3}$. The last component of DIAM is a two-layer multilayer perceptron (MLP) classifier to learn illicit probability p_v of node v . Note that DIAM in Figure 2 is an end-to-end classification framework, meaning that all modules in DIAM are jointly trained to minimize a binary cross-entropy loss formulated in Section IV-D.

B. Edge2Seq: Learn via Directed Parallel Edges

Obtaining high-quality node representations is crucial for the illicit account detection task in Section III-B. However, as mentioned in Section I, the native node features of illicit accounts are often falsified or lacking in transaction networks, since these accounts intend to pretend themselves to be benign and hide themselves among normal nodes, particularly on cryptocurrencies that are decentralized and pseudo-anonymous [8]. Existing solutions mostly resort to manual feature engineering to get statistical features [7], [10], which requires domain expertise and is dependent on a specific cryptocurrency.

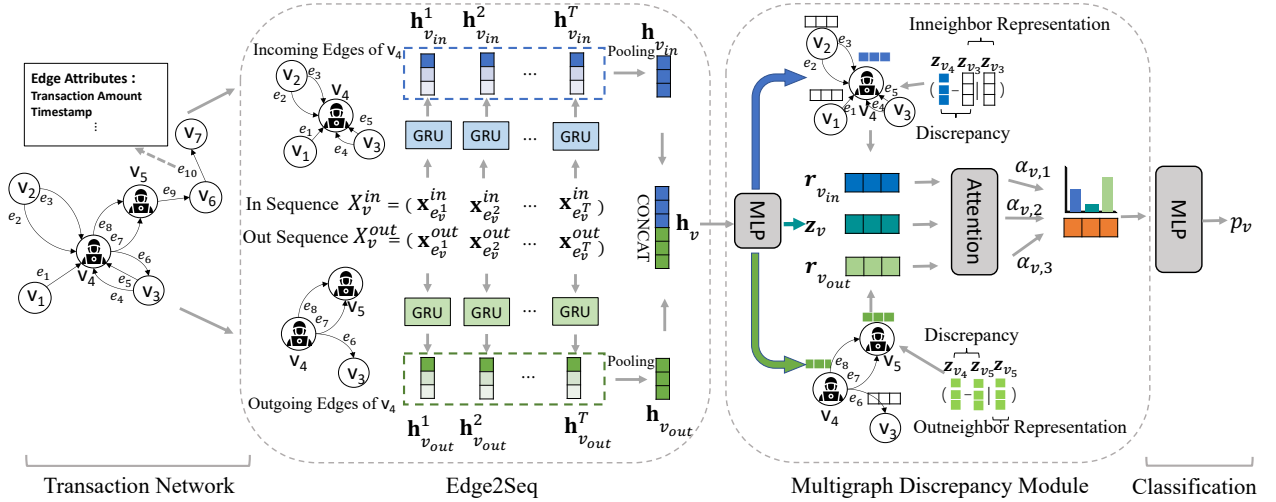


Fig. 2. The DIAM framework with an input transaction network modeled as a directed multigraph with edge attributes.

Hence, we present Edge2Seq to automatically learn high-quality node representations that preserve the intrinsic transaction patterns of nodes. In a nutshell, Edge2Seq integrates (i) edge attributes (transaction information), (ii) parallel edge sequential dependencies (transaction dependencies), and (iii) edge directions (directional transaction flows) together in the multigraph data model. Existing methods [30], [46] use RNNs as node representation aggregator, which is different from Edge2Seq that works on *edge attributes and sequential dependencies among directed parallel edges* on multigraphs.

Remark that Edge2Seq handles the incoming and outgoing edges of a node separately. In fact, the incoming and outgoing edges of a node indicate different money flow directions, whose differences are crucial to distinguish transaction patterns in cryptocurrency transaction networks [15]. For example, Chen *et al.*, [8] find that phishing accounts in Ethereum usually have fewer incoming edges, while having more outgoing edges, compared with non-phishing accounts. In addition, phishing accounts often receive 3 times more cryptocurrency amount than the amount spent.

Hence, a model should be able to differentiate and capture such directional transaction patterns. Specifically, for every node v of the input multigraph G , we first build an incoming (resp. outgoing) sequence that consists of its incoming (resp. outgoing) edge attributes ordered by timestamps. We then apply GRUs over the sequences to learn representations that preserve both edge attributes (*i.e.*, transaction information) and sequential dependencies among edges (*i.e.*, transaction behaviors). The sequence representations are then processed as the respective node representations for subsequent training. In the following, we explain the details of Edge2Seq that contains two parts: sequence generation and sequence encoding.

Sequence Generation. Given a node v of the input multigraph G , Edge2Seq first builds two sequences for it. In particular, for all outgoing edges of v , Edge2Seq sorts the outgoing edges in chronological order according to the timestamps on edges, and gets $E_v^{out} = (e_v^1, e_v^2, \dots, e_v^T)$, the sequence of T sorted outgoing edges of v . For instance, in Figure 1, node v_4 has outgoing

edge sequence (e_6, e_7, e_8) . Edge2Seq then extracts the corresponding edge attributes accordingly, and builds the outgoing edge attribute sequence of v , $X_v^{out} = (\mathbf{x}_{e_v^1}, \mathbf{x}_{e_v^2}, \dots, \mathbf{x}_{e_v^T})$. Then, similarly, we also build an incoming edge attribute sequence X_v^{in} . Obviously, sequences X_v^{out} and X_v^{in} of node v consider both edge sequence and edge attributes, and also utilize parallel edges between v and its neighbors. Intuitively, X_v^{out} (resp. X_v^{in}) represents the transaction behaviors of node v when v serves as a sender (resp. receiver).

Note that an account can participate in thousands of transactions, resulting to substantially long sequences. The number of transactions of accounts commonly follows the power-law distribution [47]. In other words, in practice, only a few nodes have too long sequences X_v^{out} or X_v^{in} . To reduce the computational costs incurred when handling extremely long sequences, we apply a common trick [23], [48], and limit the sequence length to be at most T_{max} , by keeping the most recent edges. In experiments, we study the effect of T_{max} when varying it. In addition, for nodes without any incoming or outgoing edges, we add self-loops to generate sequences.

Learning Representations by Sequence Encoding. After generating sequences X_v^{out} and X_v^{in} for node v in the input multigraph G , we adopt GRUs to learn deep sequential representations. We use node v 's length- T outgoing sequence $X_v^{out} = (\mathbf{x}_{e_v^1}, \mathbf{x}_{e_v^2}, \dots, \mathbf{x}_{e_v^T})$ to explain the encoding process, and the encoding process of X_v^{in} naturally follows. In particular, as shown in Eq. (2), starting from $t = 1$, until the end of the length- T sequence X_v^{out} , we first apply a linear transformation on edge attributes $\mathbf{x}_{e_v^t}$ to get $\mathbf{z}_{e_v^t}^{out}$ via a one-layer MLP with learnable parameters \mathbf{W}_{out} and \mathbf{b}_{out} . Then we apply GRU over $\mathbf{z}_{e_v^t}^{out}$ and the $(t-1)$ -th hidden state $\mathbf{h}_{v_{out}}^{t-1}$, to get the updated $\mathbf{h}_{v_{out}}^t$ at the t -th position of sequence X_v^{out} :

$$\begin{aligned} \mathbf{z}_{e_v^t}^{out} &= \mathbf{W}_{out} \mathbf{x}_{e_v^t} + \mathbf{b}_{out}, \\ \mathbf{h}_{v_{out}}^t &= \text{GRU}_{out}(\mathbf{z}_{e_v^t}^{out}, \mathbf{h}_{v_{out}}^{t-1}), \end{aligned} \quad (2)$$

where $\mathbf{W}_{out} \in \mathbb{R}^{\frac{c}{2} \times d}$ and $\mathbf{b}_{out} \in \mathbb{R}^{\frac{c}{2}}$ are learnable parameters, and c is the representation dimension. By convention, the initial hidden state of GRU, $\mathbf{h}_{v_{out}}^{t=0}$, is set to be zero.

Essentially, we use GRUs to generate a representation $\mathbf{h}_{v_{out}}^t$ for each outgoing edge at position $t \in [1, T]$ of sequence X_v^{out} . Then we apply element-wise max-pooling [30], [49] to get the representation $\mathbf{h}_{v_{out}}$ of sequence X_v^{out} ,

$$\mathbf{h}_{v_{out}} = \varphi_{pool} \forall t \in [1, T] (\mathbf{h}_{v_{out}}^t), \quad (3)$$

where $\varphi_{pool}(\cdot)$ is the max-pooling operation.

We apply the same procedure over the incoming sequence X_v^{in} of node v by using another GRU_{in}, to get the incoming sequence representation $\mathbf{h}_{v_{in}}$. Finally, we obtain the representation \mathbf{h}_v of node v by concatenating $\mathbf{h}_{v_{in}}$ and $\mathbf{h}_{v_{out}}$ in Eq. (4). Since we obtain $\mathbf{h}_{v_{in}}$ and $\mathbf{h}_{v_{out}}$ based on the incoming and outgoing edge attribute sequences of v respectively, inherently node representation \mathbf{h}_v can preserve the hidden transaction patterns of node v in both directions:

$$\mathbf{h}_v = \mathbf{h}_{v_{out}} \parallel \mathbf{h}_{v_{in}}. \quad (4)$$

C. MGD: Capture Discrepancies in Multigraph Topology

Note that the node representation \mathbf{h}_v of v obtained by Edge2Seq in Section IV-B only captures v 's individual transaction features contained in its outgoing and incoming edges, without considering multi-hop multigraph topology. Existing studies try to exploit graph topology and employ GNNs for better performance [8], [13], [15]. However, as explained, conventional GNNs heavily rely on the assumption that similar nodes tend to connect to each other and share similar representations [30], which may be less effective on the task of illicit account detection on multigraphs. On the other hand, an effective model should be able to learn distinguishable representations between normal and illicit nodes that may be closely connected either intentionally via camouflaging behaviors or unintentionally. Simply adoption of conventional GNNs may result to entangled representations between normal and illicit nodes, leading to suboptimal effectiveness [19], [34].

Therefore, we present a new Multigraph Discrepancy module (MGD) to address the issue. MGD consists of three technical designs: (i) directed discrepancy-aware message passing with sum pooling, (ii) layer-wise learnable transformations, and (iii) an attention mechanism over directional representations, to learn expressive representations. MGD is discrepancy-aware, in the sense that, it transforms and passes not only node representations but also the discrepancies between nodes via a carefully designed message passing mechanism on multigraphs. Furthermore, given a target node v , MGD considers the discrepancies of its incoming and outgoing neighbors separately, since a node can behave differently when being either a sender or a receiver of transactions. As validated in our experiments, MGD is highly expressive to learn distinguishable representations for illicit account detection, when compared with existing counterparts.

In DIAM, let L be the total number of MGD modules stacked together. The first MGD layer takes the representations \mathbf{h}_v of nodes $v \in V$ learned by Edge2Seq in Section IV-B as input. Without ambiguity, let $\mathbf{h}_v^{(\ell=0)}$ represent the input of the first MGD layer. As shown in Eq. (5), the ℓ -th MGD first applies a layer-wise linear transformation with learnable weights $\mathbf{W}_2^{(\ell)}$ and $\mathbf{b}_2^{(\ell)}$ to convert representation $\mathbf{h}_v^{(\ell-1)}$ to

intermediate $\mathbf{z}_v^{(\ell)}$ via a one-layer MLP. Then for an in-neighbor $u \in N_{in}(v)$, the message passed from u to v in the ℓ -th MGD is $\mathbf{W}_3^{(\ell)}(\mathbf{z}_u^{(\ell)} \parallel (\mathbf{z}_v^{(\ell)} - \mathbf{z}_u^{(\ell)}))$, which includes both in-neighbor u 's representation $\mathbf{z}_u^{(\ell)}$ and its discrepancy $(\mathbf{z}_v^{(\ell)} - \mathbf{z}_u^{(\ell)})$ with target node v , followed by a learnable linear transformation using $\mathbf{W}_3^{(\ell)}$. Aggregating all such information for every $u \in N_{in}(v)$, we obtain $\mathbf{r}_{v_{in}}^{(\ell)}$ that is the *discrepancy-aware incoming message* that node v receives from its incoming neighborhood. Note that $N_{in}(v)$ is a multiset of node v 's in-neighbors in the input multigraph G , and thus, we consider parallel edges during the message passing. Similarly, we can get the *discrepancy-aware outgoing message* $\mathbf{r}_{v_{out}}^{(\ell)}$ that v receives from its outgoing neighborhood $N_{out}(v)$, as shown in Eq. (5). Specifically, $\mathbf{r}_{v_{out}}^{(\ell)}$ considers every out-neighbor u 's representation as well as its discrepancy with v . Finally, we develop an attention mechanism to integrate the three aspects, namely v 's representation $\mathbf{z}_v^{(\ell)}$, discrepancy-aware incoming and outgoing messages $\mathbf{r}_{v_{in}}^{(\ell)}$ and $\mathbf{r}_{v_{out}}^{(\ell)}$, via attention $\alpha_{v,1}$, $\alpha_{v,2}$, and $\alpha_{v,3}$, to get node representation $\mathbf{h}_v^{(\ell)}$ at the ℓ -th MGD.

$$\begin{aligned} \mathbf{z}_v^{(\ell)} &= \mathbf{W}_2^{(\ell)} \mathbf{h}_v^{(\ell-1)} + \mathbf{b}_2^{(\ell)}, \\ \mathbf{r}_{v_{in}}^{(\ell)} &= \sum_{\forall u \in N_{in}(v)} \mathbf{W}_3^{(\ell)}(\mathbf{z}_u^{(\ell)} \parallel (\mathbf{z}_v^{(\ell)} - \mathbf{z}_u^{(\ell)})), \\ \mathbf{r}_{v_{out}}^{(\ell)} &= \sum_{\forall u \in N_{out}(v)} \mathbf{W}_3^{(\ell)}(\mathbf{z}_u^{(\ell)} \parallel (\mathbf{z}_v^{(\ell)} - \mathbf{z}_u^{(\ell)})), \\ \mathbf{h}_v^{(\ell)} &= \alpha_{v,1} \mathbf{z}_v^{(\ell)} + \alpha_{v,2} \mathbf{r}_{v_{in}}^{(\ell)} + \alpha_{v,3} \mathbf{r}_{v_{out}}^{(\ell)}, \end{aligned} \quad (5)$$

where $N_{in}(v)$ and $N_{out}(v)$ are the multisets of v 's incoming and outgoing neighbors respectively; $\mathbf{W}_2^{(\ell)} \in \mathbb{R}^{c \times c}$, $\mathbf{b}_2^{(\ell)} \in \mathbb{R}^c$, and $\mathbf{W}_3^{(\ell)} \in \mathbb{R}^{c \times 2c}$ are learnable parameters; $\alpha_{v,1}$, $\alpha_{v,2}$, and $\alpha_{v,3}$ are attention weights.

Attentions $\alpha_{v,1}$, $\alpha_{v,2}$, and $\alpha_{v,3}$ are calculated by Eq. (6). A larger attention weight indicates that the corresponding aspect is more important in the message passing process, which provides a flexible way to aggregate the messages in Eq. (5).

$$\begin{aligned} w_{v,1} &= \sigma(\mathbf{z}_v^{(\ell)} \cdot \mathbf{q}); w_{v,2} = \sigma(\mathbf{r}_{v_{in}}^{(\ell)} \cdot \mathbf{q}); w_{v,3} = \sigma(\mathbf{r}_{v_{out}}^{(\ell)} \cdot \mathbf{q}), \\ \alpha_{v,k} &= \text{softmax}((w_{v,1}, w_{v,2}, w_{v,3}))_k, \end{aligned} \quad (6)$$

where σ is the LeakyReLU activation function, $\mathbf{q} \in \mathbb{R}^c$ is the learnable attention vector, softmax is a normalization function, and $k = 1, 2, 3$.

Discussion. There are several ways to handle the discrepancy issue in literature. Here we discuss the technical differences of MGD compared with existing work [19]–[21], [34], [39]. Moreover, we experimentally compare MGD with these methods in Section V. The first way is to design new GNN layers that are able to distinguish the discrepancies between neighboring nodes, *e.g.*, GDN in AEGIS [34], FRAUDRE [39], and the proposed MGD in this section. The GNN layer (dubbed as FRA) in FRAUDRE (Eq. (2) in [39]) does not have the latter two designs in MGD and uses mean pooling. As analyzed in [50], sum pooling yields higher expressive power than mean pooling, particularly for *multiset* neighborhoods of multigraphs in this paper. Further, the attention mechanism and learnable layer-wise transformations in MGD enable the flexible pass and aggregation of both incoming and outgoing discrepancy-aware messages along parallel edges. Thus, MGD

Algorithm 1 DIAM

Input: A directed multigraph G , the set of observed node labels $Y_{\mathcal{L}}$, the set of unobserved node labels $Y_{\mathcal{U}}$, the number of MGD layers L , the number of training epochs J , batch size b

Output: Predicted labels of unobserved nodes in $Y_{\mathcal{U}}$

- 1: Initialize model parameters Θ ;
- 2: Generate incoming and outgoing edge attribute sequences X_v^{in} and X_v^{out} for nodes v in G ;
- 3: **for** $j \leftarrow 1, \dots, J$ **do**
- 4: Randomly split target nodes $Y_{\mathcal{L}}$ into batches \mathcal{B} with batch size b ;
- 5: **for** each batch \mathcal{B} **do**
- 6: Randomly sample L -hop neighbors of all target nodes in \mathcal{B} and add them into \mathcal{B}
- 7: Use Edge2Seq to get \mathbf{h}_v for nodes v in \mathcal{B} (Sect. IV-B);
- 8: **for** $\ell \leftarrow 1, \dots, L$ **do**
- 9: Get $\mathbf{h}_v^{(\ell)}$ for target nodes $v \in \mathcal{B}$ by MGD (Sect. IV-C);
- 10: **end for**
- 11: Get the predicted illicit probability p_v of target nodes v in \mathcal{B} by Eq.(7)
- 12: Compute Loss(Θ) by Eq.(8);
- 13: Update Θ through back-propagation;
- 14: **end for**
- 15: **end for**
- 16: **Return:** Predict labels for unobserved $Y_{\mathcal{U}}$;

is technically different from FRAUDRE. In [34], GDN *only* aggregates the representation differences between a target node and its neighbors, while *omitting* neighbor representations themselves (Eq. (1) and (2) in [34]). Contrarily, our MGD passes richer messages containing *both* neighbor discrepancies and neighbor representations. In addition to designing new GNN layers, there are also different methodologies in [19]–[21]. In [19], [20], they train samplers to identify discrepant neighbors, *e.g.*, via reinforcement learning in [19]. DCI [21] adopts self-supervised learning and clustering to decouple representation learning and classification. In experiments, DIAM outperforms these existing methods for illicit account detection on directed multigraphs with edge attributes. Moreover, in Section V-C, we replace our MGD in DIAM by FRA [39] and GDN [34], and compare their performance (Figure 3). The results indicate that DIAM with MGD achieves the best performance, which further validates that MGD is effective and is different from the existing techniques above.

D. Objective and Algorithm

DIAM works in an end-to-end manner to detect illicit accounts on directed multigraphs with edge attributes. At the last L -th MGD layer of DIAM, we get the final representations $\mathbf{h}_v^{(L)}$ of nodes v . For all labeled nodes v , we send their representations into a binary classifier, which is a 2-layer MLP network with a sigmoid unit as shown in Eq. (7), to generate the illicit probability p_v of a node v . Obviously, $1 - p_v$ is the normal probability of node v .

$$p_v = \text{sigmoid}(\text{MLP}(\mathbf{h}_v^{(L)})) \quad (7)$$

We adopt a binary cross-entropy loss for training,

$$\text{Loss}(\Theta) = - \sum_{y_v \in Y_{\mathcal{L}}} (y_v \log(p_v) + (1 - y_v) \log(1 - p_v)), \quad (8)$$

where $Y_{\mathcal{L}}$ is the set of groundtruth node labels, y_v is the label of node v , Θ contains all parameters of DIAM.

We employ Adam optimizer and mini-batch training [30]. Algorithm 1 presents the pseudo code of DIAM for training. At Line 1, we initialize model parameters Θ by Xavier initialization. Then at Line 2, we generate the incoming and outgoing edge attribute sequences X_v^{in} and X_v^{out} for nodes v in G , for later usage. From Lines 3 to 15, we use mini-batch training to train DIAM by J epochs. In every epoch, at Line 4, we first split target nodes with observed labels in $Y_{\mathcal{L}}$ into batches with batch size b . Then for each batch \mathcal{B} (Line 5), we first sample the L -hop neighbors of each target node in \mathcal{B} and add the sampled neighbors into the batch (Line 6). For each hop, following convention [30], we randomly sample a fixed-size set of neighbors. The sample size per hop is explained in experiments. Then at Line 7, we apply Edge2Seq to get \mathbf{h}_v for every node v in \mathcal{B} based on Section IV-B, and then from Lines 8 to 10, we use L stacked MGD modules in Section IV-C to get the discrepancy-aware representations $\mathbf{h}_v^{(L)}$ of all target node $v \in \mathcal{B}$, which are then used to calculate the illicit probabilities p_v (Line 11) and training loss (Line 12). Then model parameters are updated by back propagation at Line 13. After training the model, Algorithm 1 returns the predicted labels for unobserved nodes in $Y_{\mathcal{U}}$ as results at Line 16.

Time Complexity. We provide the time complexity analysis of DIAM. In Edge2Seq, the time complexities of one-layer MLP transformation, GRU, max-pooling are $\mathcal{O}(T_{\max}|V|dc)$, $\mathcal{O}(T_{\max}|V|c^2)$, and $\mathcal{O}(T_{\max}|V|c)$ respectively, where T_{\max} is the maximum sequence length, $|V|$ is the number of nodes, d and c are the dimensions of edge attributes and hidden representations. The overall time complexity of Edge2Seq is $\mathcal{O}(T_{\max}|V|c(c + d))$. In MGD, the time complexity of message passing operation on incoming and outgoing neighbors is the same as vanilla message passing-based GNNs like Sage [30] and GAT [17], which is $\mathcal{O}(|V|c^2 + |E|c)$, where $|E|$ is the number of edges. The time complexity of attention mechanism is $\mathcal{O}(|V|c)$, and the time complexity of the two-layer MLP is $\mathcal{O}(|V|(c^2 + 2c))$. Combining the time of all above components, we get the time complexity of DIAM as $\mathcal{O}(T_{\max}|V|c(c + d) + |E|c)$.

V. EXPERIMENTS

We experimentally evaluate DIAM against 14 baselines on 4 real-world transaction networks of cryptocurrency datasets, with the aim to answer the following 5 research questions:

- **RQ1:** How does DIAM perform in terms of effectiveness, compared with existing state of the art?
- **RQ2:** How does the MGD module perform, compared with existing counterparts?
- **RQ3:** How does the Edge2Seq module perform, compared with manual feature engineering?
- **RQ4:** How is the training efficiency of DIAM?
- **RQ5:** How does DIAM perform in sensitivity analysis?

A. Experimental Setup

Datasets. We evaluate on 4 real cryptocurrency datasets, including 2 Ethereum datasets and 2 Bitcoin datasets. The

TABLE II
STATISTICS OF THE DATASETS.

Dataset	#Nodes	#Edges	#Edge attribute	#Illicit	#Normal	Illicit:Normal
Ethereum-S [51]	1,329,729	6,794,521	2	1,660	1,700	1:1.02
Ethereum-P [8]	2,973,489	13,551,303	2	1,165	3,418	1:2.93
Bitcoin-M [52]	2,505,841	14,181,316	5	46,930	213,026	1:4.54
Bitcoin-L	20,085,231	203,419,765	8	362,391	1,271,556	1: 3.51

statistics of the datasets are listed in Table II. The first three datasets are from existing works, and we create the last largest Bitcoin dataset with more than 20 million nodes and 203 million edges. We obtain ground-truth labels into the datasets by crawling illicit and normal account labels from reliable sources, including Etherscan [44] and Wallet-Explorer [43]. Ethereum-S [51] and Ethereum-P [8] are two Ethereum transaction networks. In both datasets, every edge has two attributes: transaction amount and timestamp. The labeled illicit nodes are the addresses that conduct phishing scams in these two datasets. For Ethereum-P dataset from [8], it only contains illicit node labels. We enhance the dataset by identifying the benign accounts (*e.g.*, wallets and finance services) in Ethereum-P from Etherscan [44] as normal node labels. Bitcoin-M [52] is a medium-sized dataset containing the first 1.5 million transactions from June 2015. As explained in Section III-A, a Bitcoin transaction can involve multiple senders and receivers. After built as a multigraph, Bitcoin-M has about 2.5 million nodes and 14 million edges. In Bitcoin-M, an edge has 5 attributes: input amount, output amount, number of inputs, number of outputs, and timestamp. We build the largest Bitcoin-L based on all transactions happened from June to September 2015. Bitcoin-L has more than 20 million nodes and 200 million edges, and each edge has 8 attributes: input amount, output amount, number of inputs, number of outputs, fee, total value of all inputs, total value of all outputs, and timestamp. We obtain the labeled data in Bitcoin-M and Bitcoin-L by crawling from WalletExplorer [43]. Bitcoin addresses belonging to gambling and mixing services are regarded as illicit accounts, while the addresses in other types are normal accounts. Parallel edges between nodes are common in the datasets. For instance, in Ethereum-P, there are 5,353,834 connected node pairs, and 1,287,910 of them have more than one edge (24.06%).

Baselines. To comprehensively evaluate our method, we compare with 14 competitors in 3 categories.

- *Cryptocurrency illicit account detection methods*, including Pdetector [8], SigTran [10], and EdgeProp [15]. In particular, Pdetector leverages GCN and autoencoder to detect Ethereum phishing scams. SigTran employs feature engineering and node2vec [26] to learn node representations that are used to train a logistic regression classifier for illicit account detection. EdgeProp also uses handcrafted features to train a GNN model to identify illicit accounts.
- *Graph-based anomaly detection methods*, including CARE-GNN [19], DCI [21], PC-GNN [38], GDN from AEGIS [34], and FRAUDRE [39]. As a message passing module in AEGIS, GDN modifies GAT by using feature differences between neighboring nodes in message passing and attention mechanism, to address the discrepancy issue discussed in

Section IV-C. Note that AEGIS itself is unsupervised, which is different from the supervised setting in this paper, and thus it is not compared. DCI decouples node representation learning and anomaly detection classification, and adopts self-supervised learning for anomaly detection. CARE-GNN is based on reinforcement learning for anomaly detection on relation graphs. PC-GNN develops node sampler to alleviate class imbalance of fraud detection. FRAUDRE considers neighborhood differences and also develops a loss function to remedy class imbalance. CARE-GNN, PC-GNN, and FRAUDRE are designed for relation graphs, and we set the number of relations as 1, to run them on the datasets.

- *GNN models*, including GCN [16], Sage [30], GAT [17], GATE [17], GINE [32], and TransConv [33]. GCN is widely used to learn node representations via graph convolutions. Sage is a general inductive framework to learn embeddings by sampling and aggregating local neighborhood features. GAT employs self-attention to assign importance to neighbors, and GATE extends GAT by edge attributes. GINE also uses edge attributes for message passing. TransConv is a graph transformer network.

Since all baselines require initial node features as input, following the way in SigTran [10], we obtain node features, such as node degree and total received/sent amount, by feature engineering for the baselines. Particularly, in this way, we get 48, 48, 69, and 89 node features for datasets Ethereum-P, Ethereum-S, Bitcoin-M, and Bitcoin-L respectively. In terms of Pdetector, we extract the 8 specific node features suggested in its paper [8] for its training, in order to make a fair comparison. GDN, EdgeProp, as well as the GNN-based models, are not originally designed for the binary classification task in this paper. Therefore, we regard them as the encoder to generate node representations, which are then sent to a 2-layer MLP classifier with the same objective in Section IV-D.

Implementation Details. We implement DIAM and GNN-based models using Pytorch and Pytorch Geometric. We also use Pytorch to implement GDN and Pdetector following the respective papers. For the other competitors, we use their original codes provided by the respective authors. All experiments are conducted on a Linux server with Intel Xeon Gold 6226R 2.90GHz CPU and an Nvidia RTX 3090 GPU card.

Parameter Settings. We set node representation dimension ($c = 128$), the number of GNN layers (2), learning rate (0.001), dropout rate (0.2). In DIAM, we set maximum sequence length $T_{max} = 32$. We will study the impact of T_{max} in Section V-F. For all methods, we adopt Adam optimizer, mini-batch training [30] with batch size 128, and, if not specified, rectified linear units (ReLU) is used as the activation function. For all GNN models, GDN, EdgeProp, and our method that require neighborhood sampling, given a target

TABLE III
OVERALL RESULTS ON ALL DATASETS (IN PERCENTAGE %). **BOLD**: BEST. UNDERLINE: RUNNER-UP. RELATIVE IMPROVEMENTS BY DIAM OVER RUNNER-UPS IN BRACKETS.

Method	Ethereum-S				Ethereum-P				Bitcoin-M				Bitcoin-L			
	Precision	Recall	F1	AUC	Precision	Recall	F1	AUC	Precision	Recall	F1	AUC	Precision	Recall	F1	AUC
GCN	81.21	<u>96.35</u>	88.09	87.52	86.07	80.15	82.97	87.98	79.90	81.21	80.49	88.33	80.11	83.35	81.68	88.72
Sage	<u>92.92</u>	89.95	<u>91.39</u>	<u>91.71</u>	<u>90.49</u>	91.14	<u>90.81</u>	94.04	<u>87.17</u>	<u>83.27</u>	<u>85.16</u>	<u>90.28</u>	83.16	<u>84.79</u>	<u>83.92</u>	<u>89.93</u>
GAT	85.99	93.55	89.60	89.52	85.11	85.37	85.06	90.23	86.16	81.45	83.71	89.27	79.45	65.73	71.80	80.44
GATE	66.49	90.66	76.70	73.62	88.66	85.41	86.98	90.95	71.28	67.06	68.96	80.52	67.76	36.86	47.58	65.87
GINE	75.65	88.63	81.58	80.66	82.45	81.75	82.02	88.07	64.68	61.88	63.14	77.17	70.06	55.45	61.70	74.27
TransConv	90.97	86.16	88.47	89.00	84.92	91.25	87.95	93.03	70.55	56.43	62.62	75.61	73.93	64.09	68.52	78.79
GDN	85.55	83.79	84.63	85.14	82.42	84.00	83.19	89.13	81.56	74.76	77.99	85.51	73.68	45.92	56.57	70.62
CARE-GNN	79.81	88.53	83.93	83.61	72.72	82.76	77.41	86.42	33.41	71.93	45.36	70.04	31.02	73.29	43.57	63.50
DCI	71.77	92.18	80.71	78.86	75.44	76.95	76.19	84.47	82.19	51.47	63.30	74.50	81.18	51.77	62.53	73.91
PC-GNN	83.34	81.28	82.26	82.87	79.18	89.38	83.96	90.93	36.89	73.01	48.87	72.72	30.04	82.68	44.07	64.01
FRAUDRE	73.3	95.26	82.83	81.1	84.06	80.28	82.10	82.89	36.05	72.97	48.23	72.27	33.46	76.67	46.59	66.69
SigTran	87.10	93.33	90.11	90.23	69.41	55.47	61.66	73.90	75.97	52.24	61.91	74.30	<u>83.25</u>	75.22	79.03	85.45
Pdetector	79.27	91.60	84.99	84.65	82.37	83.58	82.97	88.98	80.43	58.77	67.92	77.81	77.08	52.76	62.64	74.14
EdgeProp	81.59	85.36	83.30	83.38	89.49	<u>91.78</u>	90.57	<u>94.15</u>	73.82	69.21	71.39	81.88	72.39	67.09	69.51	79.84
DIAM	97.11	96.68	96.89	96.97	94.82	92.95	93.86	95.66	92.83	90.39	91.59	94.43	97.72	95.40	96.55	97.39
	(+4.5%)	(+0.3%)	(+6.0%)	(+5.7%)	(+4.8%)	(+1.3%)	(+3.4%)	(+1.6%)	(+6.5%)	(+8.6%)	(+7.6%)	(+4.6%)	(+17.4%)	(+12.5%)	(+15.1%)	(+8.3%)

node, we randomly sample its 1 and 2-hop neighbors with sample size 25 and 10 respectively. For other settings in baselines, we follow the instructions in their respective papers. The number of training epochs is set as 30 in Ethereum-S, Ethereum-P, and Bitcoin-M, and set as 10 in Bitcoin-L.

Evaluation Settings. We adopt 4 evaluation metrics: Precision, Recall, F1 score, and Area Under ROC curve (AUC for short). All metrics indicate better performance when they are higher. For each dataset, we split all labeled nodes into training, validation, and testing sets with ratio 2:1:1. Each model is trained on the training set. When a model achieves the highest F1 score on the validation set, we report the evaluation results on the testing set as the model’s performance. For each method, we train it for 5 times and report the average value of each evaluation metric. We also study the training time in Section V-E and the impact when varying training set size as well as the percentage of illicit node labels in Section V-F.

B. Overall Effectiveness (RQ1)

Table III reports the overall results of DIAM and all competitors on all datasets. First, observe that DIAM consistently achieves the highest accuracy by all evaluation metrics over all datasets, outperforming all baselines often by a significant margin. For instance, on Ethereum-S, DIAM achieves 96.89% F1 score, while the F1 of the best competitor Sage is 91.39%, indicating a relative improvement of 6%. On Ethereum-P, DIAM has precision 94.82%, outperforming the best competitor by a relative improvement of 4.8%. On Bitcoin-M and Bitcoin-L, DIAM also achieves the highest accuracy for illicit account detection. In particular, DIAM achieves 91.59% and 96.55% F1 scores on Bitcoin-M and Bitcoin-L, 7.6% and 15.1% relatively higher than the best baselines, respectively.

Another observation is that the performance gain of DIAM is larger on the largest Bitcoin-L (e.g., 17.4% precision improvement over the best competitor SigTran as shown in Table III). The reason is that DIAM with Edge2Seq is able to take advantage of the abundant edge attributes in the multigraph of Bitcoin-L, to automatically extract informative representations for accurate detection of illicit accounts. Existing solutions,

such as SigTran, require manual feature engineering, and thus, could not effectively leverage the large-scale data to preserve the intrinsic transaction patterns of accounts. In Section V-D, we conduct an evaluation to further reveal the effectiveness of Edge2Seq, compared with handcrafted features.

The overall results in Table III demonstrate that DIAM is able to learn effective node representations that preserve the unique transaction patterns of both illicit and benign nodes, validating the effectiveness of the techniques proposed in Section IV. In particular, compared with existing solutions that rely on feature engineering, DIAM automatically learns deep representations via Edge2Seq in Section IV-B, which considers incoming and outgoing edge sequence dependencies, as well as edge attributes. Further, DIAM employs the proposed MGD layers in Section IV-C, to propagate both representations and the discrepancies between neighbors and target nodes, via an attention mechanism, so as to generate distinguishable representations for illicit accounts. All these techniques together in DIAM can leverage the rich semantics of the directed multigraph model for cryptocurrency transactions, in order to achieve superior performance.

C. Study on MGD (RQ2)

As we have discussed in Section IV-C, our MGD is different from existing work. To further test the effectiveness of MGD in DIAM, we replace MGD with different GNN layers, namely, Sage layer [30], GAT layer [48], GDN layer in AEGIS [34], and FRA layer in FRAUDRE [39], and compare their performance. All these layers are different from each other. In particular, given a target node v , Sage and GAT layers do not consider discrepancies, GDN layer only passes and aggregates the representation differences of its neighbors to it. Compared with the FRA layer, our MGD employs sum pooling, layer-wise learnable transformations, and an attention mechanism to flexibly pass and aggregate both incoming and outgoing neighbor discrepancies and neighbor representations.

We replace the MGD layers in DIAM by the existing GNN layers above, and then, in Figure 3, we report the F1 and AUC performance of DIAM with the 5 different GNN

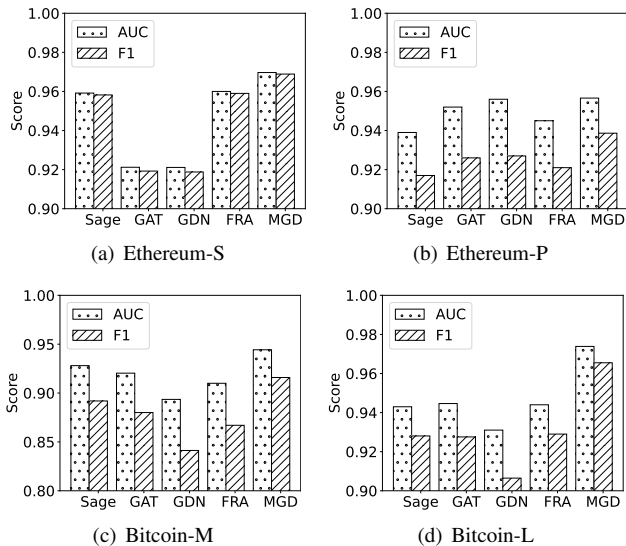


Fig. 3. Compare the MGD module with existing GNN layers including Sage, GAT, GDN, and FRA.

TABLE IV

MANUAL FEATURES V.S., LEARNED REPRESENTATIONS BY **EDGE2SEQ**: RESULTS ON BITCOIN-L WHEN APPLYING MANUAL FEATURES OR THE REPRESENTATIONS AUTOMATICALLY LEARNED BY **EDGE2SEQ** AS THE INPUT OF SAGE, GAT, AND MGD (IN PERCENTAGE %). RELATIVE IMPROVEMENTS OF **EDGE2SEQ** OVER MANUAL ARE IN BRACKETS.

GNN Layer	Variant	F1	AUC
Sage	Manual	83.92	89.93
	Edge2Seq	92.80 (+10.6%)	94.30 (+4.9%)
GAT	Manual	71.80	80.44
	Edge2Seq	92.75 (+29.2%)	94.46 (+17.4%)
MGD	Manual	85.29	92.39
	Edge2Seq	96.55 (+13.2%)	97.39 (+5.4%)

layers over all datasets. Observe that **DIAM** with MGD always achieves the highest F1 and AUC scores on all datasets, and outperforms GDN, Sage, GAT, and FRA layers. The results demonstrate the effectiveness of our MGD to preserve the differentiable representations of both illicit and benign nodes with the consideration of the discrepancies when conducting message passing over the multigraph topology. Particularly, MGD outperforms FRA due to the proposed learnable linear transformation and attention mechanism for both incoming and outgoing discrepancy-aware representations in MGD. Moreover, among existing GNN layers, GDN layer performs better than Sage, GAT, and FRA layers on Ethereum-P in Figure 3(b), while being inferior on the other three datasets. This indicates that it is also important to propagate and aggregate neighbor representations to target nodes in the input multigraph, rather than only considering node representation differences, for effective illicit account detection.

D. Study on Edge2Seq (RQ3)

The Edge2Seq technique in Section IV-B automatically learns node representations by applying GRUs over the incoming and outgoing edge sequences of nodes. On the other hand, as explained, existing solutions mostly rely on tedious feature engineering to get shallow statistical node features.

TABLE V
TRAINING TIME PER EPOCH (SECONDS)

Method	Ethereum-S	Ethereum-P	Bitcoin-M	Bitcoin-L
GCN	0.29	0.65	14.47	274.20
Sage	0.31	0.67	13.76	270.80
GAT	0.75	1.14	18.25	307.70
GATE	0.57	0.92	13.42	130.08
GINE	0.13	0.39	8.92	104.23
TransConv	0.22	0.66	14.72	181.82
EdgeProp	0.17	0.39	9.73	105.22
GDN	0.39	0.74	18.47	294.64
CARE-GNN	0.62	1.80	29.19	257.45
DCI	1.06	1.37	46.27	972.52
PC-GNN	1.62	6.10	90.70	6525.68
FRAUDRE	1.34	2.58	75.40	884.20
DIAM	0.45	0.70	35.92	330.73

We demonstrate the power of Edge2Seq by interchanging it with the handcrafted features as the input of Sage, GAT, and our MGD, and report the evaluation results on Bitcoin-L in Table IV. Specifically, in Table IV, Manual indicates to have the handcrafted node features introduced in Section V-A as the initial input of node representations for training, while Edge2Seq indicates to have the automatically learned representations by Edge2Seq for training. As shown in Table IV, comparing against Sage (resp. GAT) with manual features, Sage (resp. GAT) with Edge2Seq always achieves higher F1 and AUC by a significant margin. For instance, GAT with Edge2Seq improves GAT with manual features by a significant margin of 29.2%. The results indicate the superiority of Edge2Seq, compared with manual feature engineering. Further, the result of our MGD with manual features in Table IV (*i.e.*, **DIAM** without Edge2Seq) also indicates that Edge2Seq is important for the problem studied in this paper. Our method **DIAM** assembling Edge2Seq and MGD together obtains the best performance, as shown in Table IV.

E. Training Efficiency (RQ4)

Table V reports the average training time per epoch of **DIAM** and the competitors in seconds on all datasets. First, observe that anomaly detection methods (GDN, CARE-GNN, DCI, PC-GNN, and FRAUDRE) and our method **DIAM** are generally slower than the common GNN models listed in the first group of Table V, *e.g.*, GCN and Sage, which is because of the unique designs for illicit/anomaly detection in these methods. However, as reported in Section V-B, compared with **DIAM**, common GNN models yield inferior accuracy since they are not dedicated to the task of illicit account detection. Second, **DIAM** is faster than most graph-based anomaly detection methods. Specifically, on Ethereum-S and Ethereum-P, **DIAM** is faster than CARE-GNN, DCI, PC-GNN, and FRAUDRE. On Bitcoin-M and Bitcoin-L, **DIAM** is faster than DCI, PC-GNN, and FRAUDRE. In addition, although EdgeProp is fast, it is not as accurate as **DIAM** as shown in Section V-B. The training time per epoch in Table V does not include SigTran and Pdetector, since they are not trained in an epoch manner. Considering together the training efficiency in Table V and the effectiveness in Table III, we can conclude that **DIAM** has superior accuracy for illicit account detection, while being reasonably efficient, on large-scale datasets.

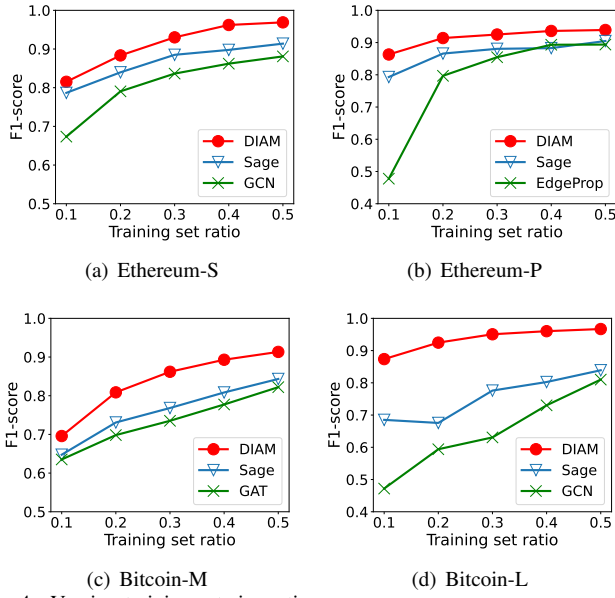
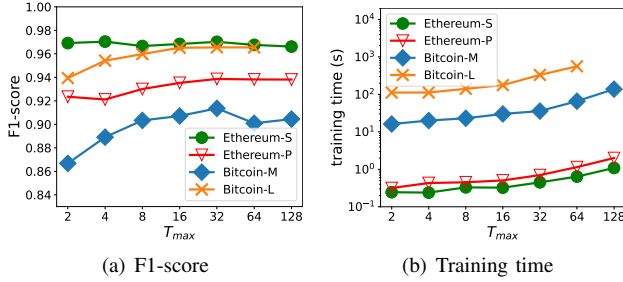


Fig. 4. Varying training set size ratio

Fig. 5. Varying T_{max}

F. Sensitivity Analysis (RQ5)

Varying training data volume. To compare the performance of DIAM with baselines under the situation with insufficient training data, we vary the percentage of training data from 10% to 50%. The F1 results on all datasets are reported in Figure 4, where DIAM and the top-2 best baselines per dataset are evaluated. The overall observation is that the F1 scores of all methods decrease as the amount of training data decrease; meanwhile, DIAM keeps achieving the highest effectiveness. On Ethereum-S in Figure 4(a), we compare DIAM with the top-2 baselines Sage and GCN of the dataset (see Table III). For different sizes of training data, DIAM keeps outperforming the baselines. Similarly, we compare DIAM with Sage and EdgeProp on Ethereum-P in Figure 4(b), compare DIAM with Sage and GAT on Bitcoin-M in Figure 4(c), compare DIAM with Sage and GCN on Bitcoin-L in in Figure 4(d). The results in all figures show that DIAM consistently achieves the highest F1 scores, regardless of the volume of training data. Another observation is that the performance of DIAM is relatively stable on the largest Bitcoin-L. Compared to training with 50% of the data, training with 10% of the data only resulted in a 9.6% decrease in model performance. While the two other competitors decreased 18.3% (Sage) and 41.7% (GCN), respectively, which validates the capability of DIAM to leverage abundant data to obtain expressive representations for illicit account detection.

TABLE VI
ABLATION STUDY (IN PERCENTAGE %)

Methods	Ethereum-S		Ethereum-P		Bitcoin-M		Bitcoin-L	
	F1	AUC	F1	AUC	F1	AUC	F1	AUC
DIAM \MGD	95.17	95.26	82.23	88.66	69.81	81.87	72.96	81.77
DIAM \A	96.75	96.83	93.28	95.62	89.94	92.93	95.36	96.65
DIAM	97.11	96.97	93.86	95.66	91.59	94.43	97.72	97.39

Varying the maximum sequence length T_{max} . We vary T_{max} in Edge2Seq from 2 to 128 and report the performance of DIAM in Figure 5(a), and average training time per epoch (seconds) in Figure 5(b). The result of $T_{max} = 128$ on Bitcoin-L is not reported due to out of GPU memory. In Figure 5(a), observe that as T_{max} increases, F1 score on Ethereum-S is relatively stable, F1 score on Ethereum-P and Bitcoin-L increases first and then becomes stable, and F1 score on Bitcoin-M increases first and then decreases after T_{max} is beyond 32. As discussed in [23], the decrease in Bitcoin-M may be caused by the noise introduced among distant elements when considering very long sequences in sequence models. Therefore, we choose $T_{max} = 32$ as default in experiments. In terms of training time per epoch in Figure 5(b), when T_{max} increases, it takes more time for training on all datasets, which is intuitive since there are longer sequences to be handled by Edge2Seq. The increasing trend of training time is consistent with the time complexity analysis in Section IV-D.

Ablation Study. To validate the effectiveness of every component in DIAM, we conduct extra ablation study by evaluating DIAM without MGD in Section IV-C (denoted as DIAM \MGD), and DIAM without the attention mechanism in Eq. (6) (*i.e.*, set $\alpha_{v,1} = \alpha_{v,2} = \alpha_{v,3} = 1$ in Eq. (5)), denoted as DIAM \A. Table VI presents their performance compared with the complete version DIAM. First, observe that the performance on all four datasets increases as we add more techniques, validating the effectiveness of the proposed MGD and attention mechanism. Further, note that essentially DIAM \MGD is only with Edge2Seq (*i.e.*, only considering a node's local transaction features), and thus, it has inferior performance as shown in Table VI. This observation indicates the importance of incorporating the multigraph topology for illicit account detection. Moreover, the effectiveness of Edge2Seq compared with manual features has been evaluated in Section V-D.

Varying illicit ratio. As shown in Table II, the number of illicit accounts is relatively high compared with normal nodes, particularly on Ethereum-S and Ethereum-P datasets. In order to stress test DIAM and the baselines when the illicit node labels are scarce, we have conducted experiments to vary the illicit ratio from 1% to 9%, by randomly sampling a subset of illicit nodes in training on every dataset. The illicit ratio is the proportion of illicit nodes in all labeled training nodes. Figure 6 reports the performance of all methods on all datasets. The overall observation is that DIAM outperforms existing methods under most illicit ratios, except the AUC at 1% on Ethereum-S. As the illicit ratio decreases, the performance of all methods drops on all datasets, since all methods would be under-trained with limited labels. Further, the superiority of DIAM is more obvious on larger datasets. The reason is that our

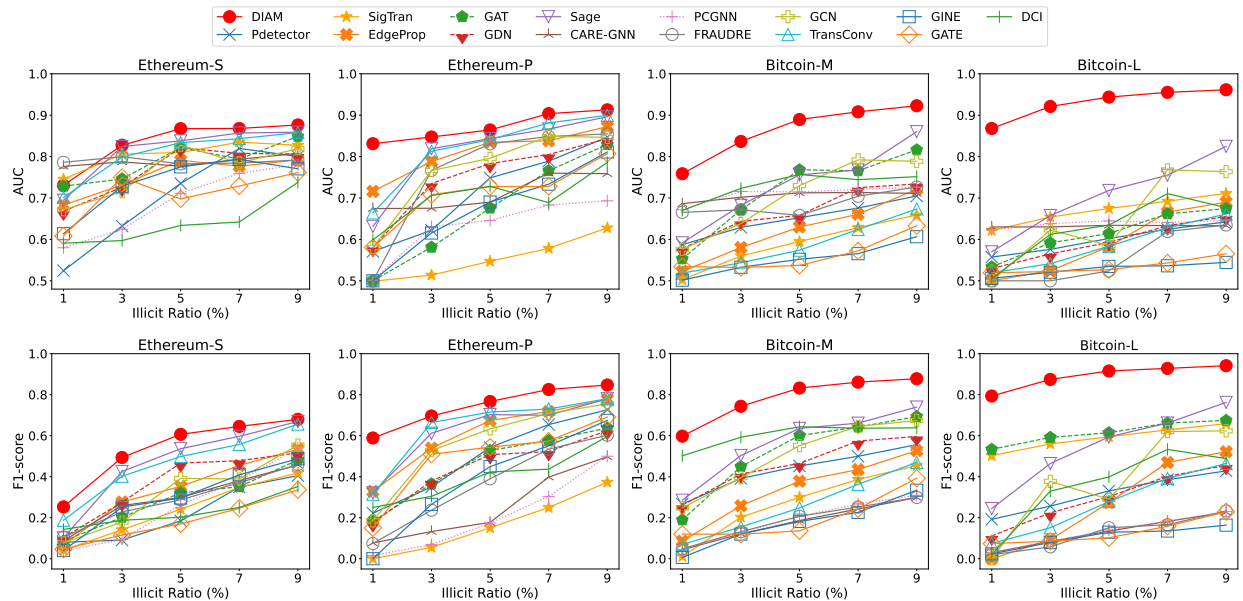


Fig. 6. Varying illicit ratio on all datasets.

method can better leverage the abundant data to automatically extract meaningful features via Edge2Seq and MGD in DIAM. The results in Figure 6 demonstrate the effectiveness of the proposed DIAM when labels are scarce.

VI. CONCLUSION

We present DIAM, an effective discrepancy-aware multi-graph neural network for the problem of illicit account detection on cryptocurrency transaction networks. The core techniques in DIAM include Edge2Seq that leverages sequence models to automatically learn node representations capturing both incoming and outgoing transaction patterns, and a new Multigraph Discrepancy module MGD, which is able to learn high-quality representations to distinguish the discrepancies between illicit and normal nodes. We conduct extensive experiments on 4 large cryptocurrency datasets, and compare DIAM against 14 existing solutions. The comprehensive experimental results show that DIAM consistently achieves superior performance. Note that the multigraph model in this paper can also describe other transaction networks besides cryptocurrencies, such as online payment data by tech firms, *e.g.*, AliPay and PayPal. Hence, in the future, in addition to cryptocurrency transaction networks, we plan to apply our method on other types of transaction networks.

REFERENCES

- [1] Alipay, "Accessible digital payments for everyone," 2023. [Online]. Available: <https://global.alipay.com/platform/site/ihome>
- [2] Paypal, "Digital wallets, money management, and more," 2023. [Online]. Available: <https://www.paypal.com/>
- [3] Wechat, "Wechat pay," 2023. [Online]. Available: <https://pay.weixin.qq.com/index.php/public/wechatpay>
- [4] Bitcoin, "Open source p2p money," 2023. [Online]. Available: <https://bitcoin.org/en/>
- [5] Ethereum, "Welcome to ethereum," 2023. [Online]. Available: <https://ethereum.org/en/>
- [6] CoinMarketCap, "Cryptocurrency prices, charts and market capitalizations," Jan 2023. [Online]. Available: <https://coinmarketcap.com/>
- [7] W. Chen, X. Guo, Z. Chen, Z. Zheng, and Y. Lu, "Phishing scam detection on ethereum: Towards financial security for blockchain ecosystem." in *IJCAI*, 2020, pp. 4506–4512.
- [8] L. Chen, J. Peng, Y. Liu, J. Li, F. Xie, and Z. Zheng, "Phishing scams detection in ethereum transaction network," *ACM TOIT*, vol. 21, no. 1, pp. 1–16, 2020.
- [9] J. Wu, Q. Yuan, D. Lin, W. You, W. Chen, C. Chen, and Z. Zheng, "Who are the phishers? phishing scam detection on ethereum via network embedding," *IEEE Transactions on Systems, Man, and Cybernetics: Systems*, 2020.
- [10] F. Poursafaei, R. Rabbany, and Z. Zilic, "Sigtran: Signature vectors for detecting illicit activities in blockchain transaction networks." in *PAKDD*, 2021, pp. 27–39.
- [11] W. Chen, Z. Zheng, J. Cui, E. Ngai, P. Zheng, and Y. Zhou, "Detecting ponzi schemes on ethereum: Towards healthier blockchain technology," in *WWW*, 2018, pp. 1409–1418.
- [12] C. G. Akcora, Y. Li, Y. R. Gel, and M. Kantarcioglu, "Bitcoinheist: Topological data analysis for ransomware prediction on the bitcoin blockchain," in *IJCAI*, 2020, pp. 4439–4445.
- [13] M. Weber, G. Domeniconi, J. Chen, D. K. I. Weidele, C. Bellei, T. Robinson, and C. E. Leiserson, "Anti-money laundering in bitcoin: Experimenting with graph convolutional networks for financial forensics," *arXiv preprint arXiv:1908.02591*, 2019.
- [14] Chainalysis, "Crypto crime trends for 2022: Illicit transaction activity reaches all-time high in value, all-time low in share of all cryptocurrency activity," Jan 2022. [Online]. Available: <https://blog.chainalysis.com/reports/2022-crypto-crime-report-introduction>
- [15] D. S. H. Tam, W. C. Lau, B. Hu, Q. F. Ying, D. M. Chiu, and H. Liu, "Identifying illicit accounts in large scale e-payment networks—a graph representation learning approach," *arXiv:1906.05546*, 2019.
- [16] T. N. Kipf and M. Welling, "Semi-supervised classification with graph convolutional networks," in *ICLR*, 2017.
- [17] P. Veličković, G. Cucurull, A. Casanova, A. Romero, P. Lio, and Y. Bengio, "Graph attention networks," *arXiv preprint arXiv:1710.10903*, 2017.
- [18] J. Zhu, Y. Yan, L. Zhao, M. Heimann, L. Akoglu, and D. Koutra, "Beyond homophily in graph neural networks: Current limitations and effective designs," *arXiv preprint arXiv:2006.11468*, 2020.
- [19] Y. Dou, Z. Liu, L. Sun, Y. Deng, H. Peng, and P. S. Yu, "Enhancing graph neural network-based fraud detectors against camouflaged fraudsters," in *CIKM*, 2020, pp. 315–324.
- [20] Z. Liu, Y. Dou, P. S. Yu, Y. Deng, and H. Peng, "Alleviating the inconsistency problem of applying graph neural network to fraud detection," in *SIGIR*, 2020, pp. 1569–1572.
- [21] Y. Wang, J. Zhang, S. Guo, H. Yin, C. Li, and H. Chen, "Decoupling representation learning and classification for gnn-based anomaly detection," in *SIGIR*, 2021, pp. 1239–1248.
- [22] K. Ding, Q. Zhou, H. Tong, and H. Liu, "Few-shot network anomaly detection via cross-network meta-learning," in *Proceedings of the Web Conference 2021*, 2021, pp. 2448–2456.

- [23] C. Liu, L. Sun, X. Ao, J. Feng, Q. He, and H. Yang, "Intention-aware heterogeneous graph attention networks for fraud transactions detection," in *ACM SIGKDD*, 2021, pp. 3280–3288.
- [24] T. Chen and C. Guestrin, "Xgboost: A scalable tree boosting system," in *ACM SIGKDD*, 2016, pp. 785–794.
- [25] G. Ke, Q. Meng, T. Finley, T. Wang, W. Chen, W. Ma, Q. Ye, and T.-Y. Liu, "Lightgbm: A highly efficient gradient boosting decision tree," *NeurIPS*, vol. 30, pp. 3146–3154, 2017.
- [26] A. Grover and J. Leskovec, "node2vec: Scalable feature learning for networks," in *ACM SIGKDD*, 2016, pp. 855–864.
- [27] X. Ma, G. Qin, Z. Qiu, M. Zheng, and Z. Wang, "Riwalk: Fast structural node embedding via role identification," in *ICDM*, 2019, pp. 478–487.
- [28] S. Li, F. Xu, R. Wang, and S. Zhong, "Self-supervised incremental deep graph learning for ethereum phishing scam detection," *arXiv preprint arXiv:2106.10176*, 2021.
- [29] J. Wang, R. Wen, C. Wu, Y. Huang, and J. Xion, "Fdgars: Fraudster detection via graph convolutional networks in online app review system," in *Companion Proceedings of The 2019 World Wide Web Conference*, 2019, pp. 310–316.
- [30] W. L. Hamilton, R. Ying, and J. Leskovec, "Inductive representation learning on large graphs," in *NeurIPS*, 2017, pp. 1025–1035.
- [31] M. McPherson, L. Smith-Lovin, and J. M. Cook, "Birds of a feather: Homophily in social networks," *Annual review of sociology*, vol. 27, no. 1, pp. 415–444, 2001.
- [32] W. Hu, B. Liu, J. Gomes, M. Zitnik, P. Liang, V. Pande, and J. Leskovec, "Strategies for pre-training graph neural networks," in *ICLR*, 2019.
- [33] Y. Shi, Z. Huang, S. Feng, H. Zhong, W. Wang, and Y. Sun, "Masked label prediction: Unified message passing model for semi-supervised classification," *arXiv preprint arXiv:2009.03509*, 2020.
- [34] K. Ding, J. Li, N. Agarwal, and H. Liu, "Inductive anomaly detection on attributed networks," in *IJCAI*, 2021, pp. 1288–1294.
- [35] I. Goodfellow, J. Pouget-Abadie, M. Mirza, B. Xu, D. Warde-Farley, S. Ozair, A. Courville, and Y. Bengio, "Generative adversarial nets," *NeurIPS*, vol. 27, 2014.
- [36] S. Zhou, Q. Tan, Z. Xu, X. Huang, and F.-I. Chung, "Subtractive aggregation for attributed network anomaly detection," in *CIKM*, 2021, pp. 3672–3676.
- [37] T. Zhao, C. Deng, K. Yu, T. Jiang, D. Wang, and M. Jiang, "Error-bounded graph anomaly loss for gnns," in *CIKM*, 2020, pp. 1873–1882.
- [38] Y. Liu, X. Ao, Z. Qin, J. Chi, J. Feng, H. Yang, and Q. He, "Pick and choose: A gnn-based imbalanced learning approach for fraud detection," in *Proceedings of the Web Conference 2021*, 2021, pp. 3168–3177.
- [39] G. Zhang, J. Wu, J. Yang, A. Beheshti, S. Xue, C. Zhou, and Q. Z. Sheng, "Fraudre: Fraud detection dual-resistant to graph inconsistency and imbalance," in *ICDM*, 2021, pp. 867–876.
- [40] J. Wu, J. Liu, Y. Zhao, and Z. Zheng, "Analysis of cryptocurrency transactions from a network perspective: An overview," *Journal of Network and Computer Applications*, p. 103139, 2021.
- [41] L. Wu, Y. Hu, Y. Zhou, H. Wang, X. Luo, Z. Wang, F. Zhang, and K. Ren, "Towards understanding and demystifying bitcoin mixing services," in *Proceedings of the Web Conference*, 2021, pp. 33–44.
- [42] Z. Zheng, S. Xie, H. Dai, X. Chen, and H. Wang, "An overview of blockchain technology: Architecture, consensus, and future trends," in *IEEE international congress on big data*, 2017, pp. 557–564.
- [43] WalletExplorer, "Walletexplorer.com: Smart bitcoin block explorer," 2023. [Online]. Available: <https://www.walletexplorer.com/>
- [44] Etherscan, "Etherscan.io - ethereum (eth) blockchain explorer," 2023. [Online]. Available: <https://etherscan.io/labelcloud>
- [45] K. Cho, B. Van Merriënboer, D. Bahdanau, and Y. Bengio, "On the properties of neural machine translation: Encoder-decoder approaches," *arXiv preprint arXiv:1409.1259*, 2014.
- [46] X. Huang, Q. Song, Y. Li, and X. Hu, "Graph recurrent networks with attributed random walks," in *ACM SIGKDD*, 2019, pp. 732–740.
- [47] T. Chen, Z. Li, Y. Zhu, J. Chen, X. Luo, J. C.-S. Lui, X. Lin, and X. Zhang, "Understanding ethereum via graph analysis," *ACM TOIT*, vol. 20, no. 2, pp. 1–32, 2020.
- [48] A. Vaswani, N. Shazeer, N. Parmar, J. Uszkoreit, L. Jones, A. N. Gomez, Ł. Kaiser, and I. Polosukhin, "Attention is all you need," in *NeurIPS*, 2017, pp. 5998–6008.
- [49] R. Zhang, H. Lee, and D. Radev, "Dependency sensitive convolutional neural networks for modeling sentences and documents," *arXiv preprint arXiv:1611.02361*, 2016.
- [50] K. Xu, W. Hu, J. Leskovec, and S. Jegelka, "How powerful are graph neural networks?" in *ICLR*, 2018.
- [51] Z. Yuan, Q. Yuan, and J. Wu, "Phishing detection on ethereum via learning representation of transaction subgraphs," in *International Conference on Blockchain and Trustworthy Systems*. Springer, 2020, pp. 178–191.
- [52] J. Wu, J. Liu, W. Chen, H. Huang, Z. Zheng, and Y. Zhang, "Detecting mixing services via mining bitcoin transaction network with hybrid motifs," *IEEE Transactions on Systems, Man, and Cybernetics: Systems*, 2021.